

A Mesoporous Metal–Organic Framework with Permanent Porosity

Xi-Sen Wang,[†] Shengqian Ma,[†] Daofeng Sun,[†] Sean Parkin,[‡] and Hong-Cai Zhou*[†]

Department of Chemistry & Biochemistry, Miami University, Oxford, Ohio 45056, and Department of Chemistry, University of Kentucky, Lexington, Kentucky 40506

Received September 13, 2006; E-mail: zhouh@muohio.edu

Recent studies in metal–organic frameworks (MOFs)¹ have focused on the construction of MOFs with permanent porosity for gas storage,² separation,³ and catalysis.⁴ These applications hinge on two important properties of MOFs: porosity and stability. So far, almost all reported open MOFs are microporous (with pore sizes <2 nm). The augmentation of their channel sizes to mesoporous range (2–50 nm) still poses a great challenge. Ligand extension is an apparent option, but open MOFs built from large ligands tend to collapse upon guest removal. The concurrent application of ligand extension and SBU stabilization from this laboratory has led to open MOFs with permanent porosity and large channels.⁵ Another difficulty in the preparation of a mesoporous MOF (mesoMOF) by ligand extension is that a MOF constructed from a large ligand is often accompanied by framework interpenetration. This can drastically reduce the size of the pores, thus limiting the entrance of large molecules to the MOF.⁶ Ways must be devised to extend the ligand while inhibiting interpenetration and reinforcing the framework against disintegration upon guest removal. The quantum leap in research along these lines is the preparation of a mesoMOF exhibiting the characteristic type IV isotherm showing pore condensation and adsorption–desorption hysteresis. This communication presents such a mesoMOF (mesoMOF-1).

Herein, we demonstrate a facile route for the synthesis of a stable mesoMOF. It involves a one-pot solvothermal synthesis, followed by stabilization at pH values around 3.0. Importantly, these novel mesoporous materials possess uniform pore sizes and thermal stability comparable to that of other MOFs. This work may provide a general entry to the synthesis of stable mesoMOFs.

The ligand 4,4',4''-s-triazine-1,3,5-triyltri-*p*-aminobenzoate (TATAB, Figure 1a)⁷ is our ligand of choice for constructing mesoMOF-1. It is more extended than other tricarboxylate ligands, such as BTC,^{1d} BTB,^{2a} and TATB.^{2c} There are three amino groups in the ligand prearranged so that they will not participate in framework formation but will accept protons after the MOF is formed, giving rise to a stable ionic mesoMOF. With the new ligand containing hierarchical functional groups, we have prepared mesoMOF-1, Cu₃(TATAB)₂(H₂O)₃·8DMF·9H₂O, and applied a series of acids to stabilize its framework, leading to permanent meso-channels.

Crystals of mesoMOF-1 were prepared in a solvothermal reaction of Cu(NO₃)₂·2.5H₂O and H₃TATAB in DMF at 90 °C. The product was isolated as blue octahedral crystals (yield: 68%).

X-ray diffraction studies from multiply twinned crystals reveal that mesoMOF-1⁸ crystallizes in cubic space group *Fm* $\bar{3}$. Two copper atoms are bridged by four carboxylates to form the well-known paddlewheel secondary building unit (SBU, Figure 1b) with axial aqua ligands. As a result of repulsions between the hydrogen atoms of the peripheral rings and those of amino groups, the TATAB ligand in mesoMOF-1 is nonplanar, with an average

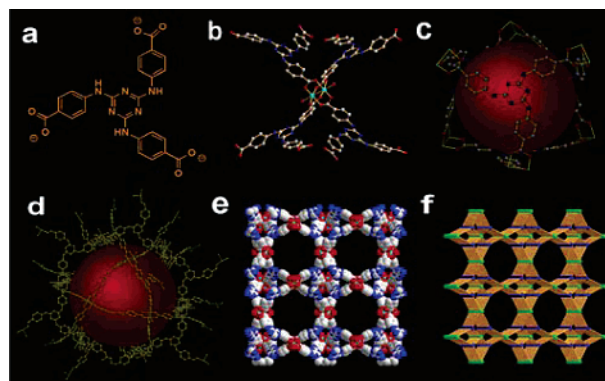


Figure 1. (a) TATAB. (b) A paddlewheel structural unit of mesoMOF-1. (c) A T_d octahedron. The red sphere represents the void inside the cage. (d) A cuboctahedral cage. The distance between opposite corners is 38.5 Å. (e) A view of packing of mesoMOF-1 from the [001] direction. (f) The augmented twisted boracite network of mesoMOF-1.

dihedral angle between central and peripheral rings of 15.8°. Each SBU connects four TATAB ligands, and each TATAB binds three SBUs to form a T_d octahedron (Figure 1c), in which all six vertices are occupied by the SBUs, and four of the eight faces are spanned by TATAB ligands. Eight such T_d octahedra occupy the eight vertices of a cube to form a cuboctahedron (Figure 1d) through corner sharing. These cuboctahedra propagate to a three-dimensional framework (Figure 1e) with a twisted boracite net topology (Figure 1f).⁹ Open channels from all three orthogonal directions are identical in size and are as large as 22.5 × 26.1 Å (atom to atom distances). MesoMOF-1 is isostructural with HKUST-1^{1d} and the single-net structure of PCN-6.^{2c} PCN-6 is interpenetrated because the planarity of TATB allows strong π – π interaction between ligands of the two interpenetrated nets. In mesoMOF-1, such π – π interactions are absent because of the nonplanarity of TATAB ligands, thus mesoMOF-1 is non-interpenetrated. In HKUST-1, BTC is planar, but the ligand is simply too small to allow interpenetration, which would cause significant steric repulsions between the two interpenetrated nets.

Because mesoMOF-1 is non-interpenetrated, high porosity can be expected: the solvent accessible volume calculated using PLATON¹⁰ is as high as 88.3%. The calculated density of mesoMOF-1 after solvent removal is as low as 0.262 g/cm³. Not surprisingly, the crystals of mesoMOF-1 lose solvent quickly once removed from the mother liquor. Thermogravimetric analysis (TGA) indicates that as-synthesized mesoMOF-1 decomposes at temperatures lower than 180 °C (Figure 2).

To stabilize the meso-channels, acids [HX, X = F, Cl, Br] have been used to react with the amino groups in TATAB to afford ionic frameworks, [Cu₃(H₃TATAB)₂(X)₃]₃X₃, or mesoMOF-1-HX, which should have higher thermal stability.

TGA studies of mesoMOF-1-HX (Figure 2, X = F[−], Cl[−], or Br[−]) indicate that these ionic frameworks are stable up to 300 °C.

[†] Miami University.

[‡] University of Kentucky.

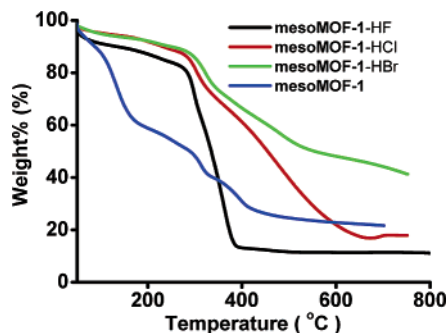


Figure 2. The TGA curves of mesoMOF-1 and mesoMOF-1-HX.

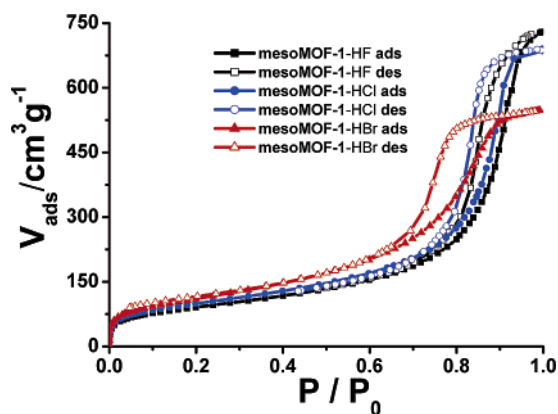


Figure 3. Gas sorption isotherms (77 K) of mesoMOF-1-HX.

After acid treatments, these compounds exhibit permanent porosity, which has been confirmed by gas sorption studies. Prior to gas sorption experiments, guest solvent molecules are removed by solvent exchange,^{2g} followed by thermal activation^{2b} under a dynamic vacuum at an optimized temperature of 80 °C. Activation at higher temperature results in a decrease in measured surface area (see Supporting Information).

The Brunauer–Emmett–Teller (BET) isotherm of mesoMOF-1-HF, shown in Figure 3, exhibits a typical type IV behavior, showing pore condensation with pronounced adsorption–desorption hysteresis. This indicates the existence of mesopores in mesoMOF-1-HF with a maximum N₂ uptake of 729 cm³/g. Similarly, HCl and HBr were used to stabilize mesoMOF-1 to prepare mesoMOF-1-HCl and mesoMOF-1-HBr, respectively. The samples also exhibit typical type IV isotherms, indicating the preservation of the ordered mesoporous structure. There is a decrease in maximum N₂ uptake (685 cm³/g for mesoMOF-1-HCl and 548 cm³/g for mesoMOF-1-HBr). The trend of the maximum N₂ uptake correlates well with the size of the X[−] anions. These BET measurements confirm that acid-treated mesoMOF-1 possesses mesoporosity. To the best of our knowledge, mesoMOF-1-HX represents the first MOF exhibiting a type IV adsorption–desorption isotherm.

In summary, by using a newly designed ligand containing hierarchical functional groups, a non-interpenetrated mesoMOF was prepared and stabilized by acid treatment. BET measurements of

the mesoMOF confirm the existence of mesopores. This mesoMOF possesses pores of uniform size and is relatively easy to make. It may have a large impact on separation and size-selective catalysis. In particular, it could become an ideal template for the preparation of monodispersed nanomaterials.¹¹

Acknowledgment. This work was supported by the National Science Foundation (CHE-0449634), Miami University, and the donors of the American Chemical Society Petroleum Research Fund. H.-C.Z. also acknowledges the Research Corporation for a Research Innovation Award and a Cottrell Scholar Award. The diffractometer was funded by NSF Grant CHE-0319176 (S.P.).

Supporting Information Available: Detailed experimental procedures, X-ray structure determination, thermogravimetric analysis, and gas adsorption data. This material is available free of charge via the Internet at <http://pubs.acs.org>.

References

- (1) (a) Kitagawa, S.; Kitaura, R.; Noro, S. *Angew. Chem., Int. Ed.* **2004**, *43*, 2334. (b) Ockwig, N. W.; Delgado-Friedrichs, O.; O'Keeffe, M.; Yaghi, O. M. *Acc. Chem. Res.* **2005**, *38*, 176. (c) Yaghi, O. M.; O'Keeffe, M.; Ockwig, N. W.; Chae, H. K.; Eddaoudi, M.; Kim, J. *Nature* **2003**, *423*, 705. (d) Chui, S. S.-Y.; Lo, S. M.-F.; Charmant, J. P. H.; Orpen, A. G.; Williams, I. D. *Science* **1999**, *283*, 1148.
- (2) (a) Chen, B.; Eddaoudi, M.; Hyde, S. T.; O'Keeffe, M.; Yaghi, O. M. *Science* **2001**, *291*, 1021. (b) Chen, B. L.; Ockwig, N. W.; Millward, A. R.; Contreras, D. S.; Yaghi, O. M. *Angew. Chem., Int. Ed.* **2005**, *44*, 4745. (c) Sun, D.; Ma, S.; Ke, Y.; Collins, D. J.; Zhou, H.-C. *J. Am. Chem. Soc.* **2006**, *128*, 3896. (d) Rowsell, J. L. C.; Yaghi, O. M. *J. Am. Chem. Soc.* **2006**, *128*, 1304. (e) Ma, S.; Zhou, H.-C. *J. Am. Chem. Soc.* **2006**, *128*, 11734. (f) Eddaoudi, M.; Kim, J.; Rosi, N.; Vodak, D.; Wachter, J.; O'Keeffe, M.; Yaghi, O. M. *Science* **2002**, *295*, 469. (g) Rowsell, J. L. C.; Eckart, J.; Yaghi, O. M. *J. Am. Chem. Soc.* **2005**, *127*, 14904. (h) Sun, D.; Ke, Y.; Mattox, T. M.; Betty, A. O.; Zhou, H.-C. *Chem. Commun.* **2005**, 5447.
- (3) (a) Matsuda, R.; Kitaura, R.; Kitagawa, S.; Kubota, Y.; Belosludov, R. V.; Kobayashi, T. C.; Sakamoto, H.; Chiba, T.; Takata, M.; Kawazoe, Y.; Mita, Y. *Nature* **2005**, *436*, 238. (b) Dinca, M.; Long, J. R. *J. Am. Chem. Soc.* **2005**, *127*, 9376. (c) Pan, L.; Adams, K. M.; Hernandez, H. E.; Wang, X.; Zheng, C.; Hattori, Y.; Kaneko, K. *J. Am. Chem. Soc.* **2003**, *125*, 3062. (d) Dytbsev, D. N.; Chun, H.; Yoon, S. H.; Kim, D.; Kim, K. *J. Am. Chem. Soc.* **2004**, *126*, 32. (e) Pan, L.; Parker, B.; Huang, X.; Olson, D. H.; Lee, J. Y.; Li, J. *J. Am. Chem. Soc.* **2006**, *128*, 4180.
- (4) (a) Kesanli, B.; Lin, W. B. *Coord. Chem. Rev.* **2003**, *246*, 305. (b) Lin, W. B. *J. Solid State Chem.* **2005**, *178*, 2486. (c) Seo, J. S.; Whang, D.; Lee, H.; Jun, S. I.; Oh, J.; Young, J.; Kim, K. *Nature* **2000**, *404*, 982. (d) Zou, R.; Sakurai, H.; Xu, Q. *Angew. Chem., Int. Ed.* **2006**, *45*, 2542. (e) Dytbsev, D. N.; Nuzhdin, A. L.; Chun, H.; Bryliakov, K. P.; Konstantin, P.; Talsi, E. P.; Fedin, V. P.; Kim, K. *Angew. Chem., Int. Ed.* **2006**, *45*, 915.
- (5) (a) Sun, D.; Ke, Y.; Mattox, T. M.; Parkin, S.; Zhou, H.-C. *Inorg. Chem.* **2006**, *45*, 7566. (b) Sun, D.; Collins, D. J.; Ke, Y.; Zuo, J.-L.; Zhou, H.-C. *Chem.—Eur. J.* **2006**, *12*, 3768.
- (6) (a) Reineke, T. M.; Eddaoudi, M.; Moler, D.; O'Keeffe, M.; Yaghi, O. M. *J. Am. Chem. Soc.* **2000**, *122*, 4843. (b) Yaghi, O. M.; Li, H.; Davis, C.; Richardson, D.; Groy, T. L. *Acc. Chem. Res.* **1998**, *31*, 474.
- (7) Pogosyan, G. M.; Zaplishnyi, V. N.; Asaturyan, I. A. *Arm. Khim. Zh.* **1977**, *30*, 342.
- (8) Crystal data for **1**: Cu₂C₃₂H₂₀N₈O₁₀, *M* = 803.64, cubic, space group *Fm* $\bar{3}$, *T* = 240(2) K, *a* = 49.6188(8) Å, *V* = 122162(3) Å³, *Z* = 24, ρ_{calc} = 0.262 g/cm³, *R*₁ = 0.0912, *wR*₂ = 0.2558.
- (9) O'Keeffe, M.; Eddaoudi, M.; Li, H. L.; Reineke, T.; Yaghi, O. M. *J. Solid State Chem.* **2000**, *152*, 3.
- (10) Spek, A. L. *J. Appl. Crystallogr.* **2003**, *36*, 7.
- (11) (a) Moon, H. R.; Kim, J. H.; Suh, M. P. *Angew. Chem., Int. Ed.* **2006**, *44*, 1261. (b) Suh, M. P.; Moon, H. R.; Lee, E. Y.; Jang, S. Y. *J. Am. Chem. Soc.* **2006**, *128*, 4710.

JA066616R